Metallogr. Microstruct. Anal. (2012) 1:85–91
DOI 10.1007/s13632-012-0017-9

TECHNICAL ARTICLE

Analysis of Design of Experiments Methodology for Optimization of Pulsed Current GTAW Process Parameters for Ultimate Tensile Strength of UNS S32760 Welds

M. Yousefieh · M. Shamanian · A. R. Arghavan

Received: 15 December 2011 / Accepted: 2 July 2012 / Published online: 26 July 2012

Abstract This work deals with the improvement of ultimate tensile strength (UTS) of super duplex stainless steel (SDSS, UNS S32760) welds fabricated by pulsed current gas tungsten arc welding (PCGTAW) process. The Taguchi method, a design of experiment technique, was employed to optimize PCGTAW process parameters to improve the UTS of SDSS weldments. The optimum conditions were found to be the second level of pulse current (120 A), second level of background current (60 A), first level of % on time (40) and second level of pulse frequency (3 Hz). Under these conditions, UTS was predicted as 776 MPa that was very close to the observed value of 769 MPa. Analysis of variance (ANOVA) was performed on the measured data and signal-to-noise ratios. As a result of ANOVA, the % on time was found to be the most significant factor affecting the UTS of SDSS welds by percentage contribution of 62.23. The pulse current (21.13%) and the background current (16.18%) had also the next most significant effects on the UTS. The pulse frequency with the 0.46% contribution was insignificant.

Keywords Stainless steel · Welding · Ultimate tensile strength · Taguchi method

M. Yousefieh (✉) · A. R. Arghavan
Department of Engineering, Islamic Azad University, Semnan Branch, Semnan, Iran
e-mail: m.yousefieh@semnaniau.ac.ir; yousefiehm@gmail.com

M. Shamanian
Department of Materials Engineering, Isfahan University of Technology, 84156-83111 Isfahan, Iran

Introduction

Super duplex stainless steels (SDSS) are corrosion-resistant alloys with high toughness and mechanical strength used in the chemical and petrochemical industries. In comparison to conventional austenitic grades (AISI 304L, 316L), SDSSs are more expensive, but exhibit higher strength levels and better pitting resistance in chloride environments [1, 2]. It has been well reported that the best mechanical and corrosion properties of duplex and super duplex steels are achieved when ferrite-to-austenite (α/γ) ratio is near to one [3] and other phases are not present. Sigma (σ) and chi (χ) phases, secondary austenite (γ_2), chromium carbides and nitrides deteriorate mechanical and corrosion properties [4].

During welding and post-weld treatments, several phase transformations can take place in the heat-affected zone (HAZ) and in the weld metal. In fact, the main concern in welding process is to obtain a α/γ ratio of one and to avoid the formation of deleterious phases such as sigma and Cr_2N during cooling and re-heating steps. The considerable presence of precipitates such as Cr_2N and sigma phase can deteriorate corrosion and mechanical properties.

Pulsed current gas tungsten arc welding (PCGTAW), developed in the 1950s, is a joining technology, which is a variant of the constant current gas tungsten arc welding (CCGTAW) process utilized in a wide range of applications [5, 6]. The PCGTAW involves cycling of the welding current from a high to a low level at a selected regular frequency. The high level of the pulse current is generally selected to give adequate penetration and bead contour, while the low level of the background current is set at a level sufficient to improve stability of arc. The PCGTAW process has many specific advantages compared to CCGTAW, such as reduced porosity, low distortion, refined grain size, enhanced arc stability, increased weld depth to

width ratio, better control of heat input, and reduction in the HAZ [7]. In general, the PCGTAW process is suitable for joining thin and medium thickness materials, e.g., stainless steel sheets, especially where metallurgical control of the weld metal is critical [8]. All these advantages will help in improving mechanical and corrosion properties. The definitions of pulse current, background current, and time duration modes are schematically illustrated in Fig. 1.

The Taguchi method is a systematic approach for design and analysis of experiments to improve the quality characteristics. The method permits evaluation of the effects of individual parameters independent of others [9–12]. Nowadays, the Taguchi method has become a practical tool for improving the quality of the output without increasing the cost of experimentation by reducing the number of experiments. This method was introduced by R. A. Fisher in the 1920s and the concept was improved in the 1940s by G. Taguchi. The aim of this method is to find out the optimal and robust process characteristic that has a minimized sensitivity to noises. It is a type of fractional factorial design which uses an orthogonal array to study the influence of factors with only a small number of experiments. The design of experiments using Taguchi method provides efficient and systematic approach to determine the optimum conditions [13, 14]. The steps of Taguchi method may be illustrated as: identification the quality characteristics and selection of design parameters, determination of the number of factor levels, selection of the appropriate orthogonal array, executing the experiments based on the arrangement of the orthogonal array, evaluating the results using signal-to-noise (S/N) ratios, analysis of variance (ANOVA), selection of the optimum levels of factors, verifying the optimum process parameters through the confirmation experiment [15].

The papers investigating the effect of pulsed current parameters on ultimate tensile strength (UTS) are very scanty. Moreover, no systematic study has been reported so far to analyze the influence of pulsed current parameters on UTS. The purpose of the present investigation is to optimize the pulsed GTAW process parameters for improvement of UTS of SDSS UNS S32760 welds using design of experiments methodology.

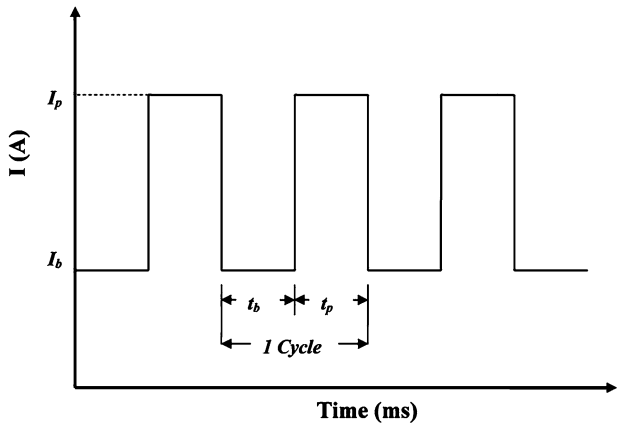

Fig. 1 Pulsed current GTAW process parameters. I_p is the pulse current (A), I_b is the background current (A), t_p is the pulse current duration (ms), t_b is the background current duration (ms), $F = 1/(t_p + t_b)$ is the pulse frequency (Hz), and % on time is the pulse current duration in one cycle

Experimental Work

In this study, UNS S32760 SDSS was received as 7-mm-thick plates. The plates were subjected to PCGTAW process using ER 2594 filler metal. High-purity argon was used as arc plasma and shielding gas with a flow rate of 10 L/min. PCGTAW process parameters were voltage of 15 V and travel speed of 100 mm/min. The chemical compositions of the base and filler materials used in this study are given in Table 1.

The samples were prepared by grinding, polishing, and etching by the following procedure:

Electrolytic etching in a KOH solution (100 mL H_2O + 15 g of potassium hydroxide), applying 3 V for 12 s. The parameters of this reagent were adjusted to reveal clearly σ phase and other deleterious phases, such as χ, γ_2, and eventually Cr_2N that precipitated in association with σ [5, 15]. The microstructures of samples were observed by scanning electron microscope (SEM) equipped with energy dispersive x-ray spectrometer (EDX) system. The x-ray count rate was estimated as 2×10^3 counts per second (cps).

The tensile strength (MPa) of the weld metal was used as an index for evaluation of mechanical properties. Because the failure must be initiated inside the weld zone,

Table 1 Chemical composition of the base and filler materials (wt.%)

Element	C	Mn	P	S	Si	Cr	Ni	Mo	N	Cu
Base metal (UNS S32760)	0.03	0.83	0.02	0.01	0.92	25.5	6.4	3.5	0.22	0.62
Filler metal (ER 2594)	0.03	0.73	0.001	0.002	0.94	25.9	9.2	4.2	0.22	0.54

1 mm × 2 mm notches were created at the center of the weld. The specimens were collected from the stable weld region by discarding the run-on and run-off portion of the weld.

The specimens for tensile strength were prepared after machining the top and root parts of the weld. In accordance with the DIN 50215 Standard (Fig. 2), the tensile test was performed at room temperature using a Houndsfield H50KS testing machine, with a maximum capacity of 60 kN under static load condition. The load was uniaxially applied on the specimens at a crosshead speed of 1 mm/min. The UTS was determined from the ratio of maximum load and original cross-sectional area of the specimens.

Taguchi Design of Experiment

The Taguchi method uses special orthogonal arrays to study all the design factors with a minimum of experiments. Orthogonality means that each factor is independently evaluated and the effect of one factor does not interfere with an estimation of the influence of another factor [9]. Four factors (pulse current, background current, % on time (the pulse current time in one cycle), pulse frequency) with three levels were selected as shown in Table 2. The factors and levels were used to design an experimental layout using an L9 (3^4) array.

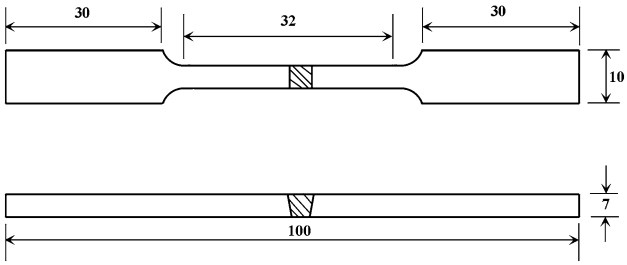

Fig. 2 Schematic diagram showing the dimensions of tensile specimen obtained by machining (all dimensions are in mm) with a notch of 1 mm × 2 mm at the weld center

Table 2 Parameters and their values corresponding to their levels studied in experiments

Parameters	Code	Levels		
		1	2	3
Pulse current, A	A	100	120	140
Background current, A	B	50	60	70
% on time	C	40	60	80
Pulse frequency, Hz	D	1	3	5

Results and Discussion

ANOVA and S/N ratio analysis were conducted on the measured UTS data.

There are three categories of quality characteristics, i.e., the higher the better (HB), the lower the better (LB), and the nominal the better (NB). The performance statistics were chosen as the optimization criterion. In this study, UTS is treated as a characteristic value. Since the UTS of welds is preferred to be maximized, the S/N ratio for HB characteristics was selected, which can be calculated from the following equation [15]:

$$\mathrm{S/N} = -10\log_{10}\left(\frac{1}{n}\sum_{i=1}^{n}\frac{1}{Y_i^2}\right), \quad (1)$$

where S/N is performance statistics, defined as the signal-to-noise ratio (S/N unit: dB), n is the number of repetitions for an experimental combination, and Y_i is a performance value of the ith experiment. Table 3 shows the experimental results for UTS and the corresponding S/N ratios using Eq. (1).

The effects of parameters are calculated using an average S/N ratio for each level. The effect of background current in its second level is calculated as follows:

$$B_2 = (\mathrm{S/N}_2 + \mathrm{S/N}_5 + \mathrm{S/N}_8)/3$$

The mean S/N ratio for each level of the other parameters can be calculated in the same way. The determined factor responses are summarized in Table 4.

Rank (1) in Table 4 indicates that % on time has more significant effect on the UTS. Ranks (2) and (3) are pulse current and background current, respectively, which have less effect, while rank (4) is pulse frequency with no effect on the UTS.

Figure 3 illustrates the average S/N ratio for each parameter at three levels. As seen in Fig. 3, % on time, pulse current, and background current exhibit large variations. The variation is found to be small in the case of pulse frequency. According to the analysis, while % on time is the most effective parameter, the pulse frequency is the least effective in the PCGTAW process.

The slopes of the lines between different levels are not the same for pulse current and background current factors (see Fig. 3a, b). So, the levels have different influences on UTS. However, the slopes of the lines are almost the same for % on time and pulse frequency (see Fig. 3c, d).

As seen in Fig. 3(c), % on time is the most effective factor chosen in this study. It can be seen from the figure that the slopes of the lines between 40–60 and 60–80 are almost the same. The mean S/N ratio decreases linearly with % on time. So, the highest UTS occurred at the lowest % on time (40). This may be due to the direct effect of % on time on the formation of sigma phase. As % on time

Table 3 Experimental results for UTS and corresponding S/N ratios

Trial no.	Pulse current, A	Background current, A	% on time	Pulse frequency, Hz	UTS, MPa	S/N ratio, dB
1	100	50	40	1	584	55.3283
2	100	60	60	3	566	55.0563
3	100	70	80	5	425	52.5678
4	120	50	60	3	600	55.5630
5	120	60	80	5	581	55.2835
6	120	70	40	1	674	56.5732
7	140	50	80	5	491	53.8216
8	140	60	40	1	734	57.3139
9	140	70	60	3	552	54.8388
Average						55.1496

Table 4 The response table for S/N ratio

	Factors			
	A	B	C	D
Level 1	54.3175	54.9043	**56.4051**	55.1502
Level 2	**55.8066**	**55.8846**	55.1527	**55.1504**
Level 3	55.3248	54.6599	53.8910	55.1482
Δ (maximum − minimum)	1.4891	1.2247	2.5141	0.0021
Rank	2	3	1	4

The optimum levels of the factors are given in bold (the highest value in the column)

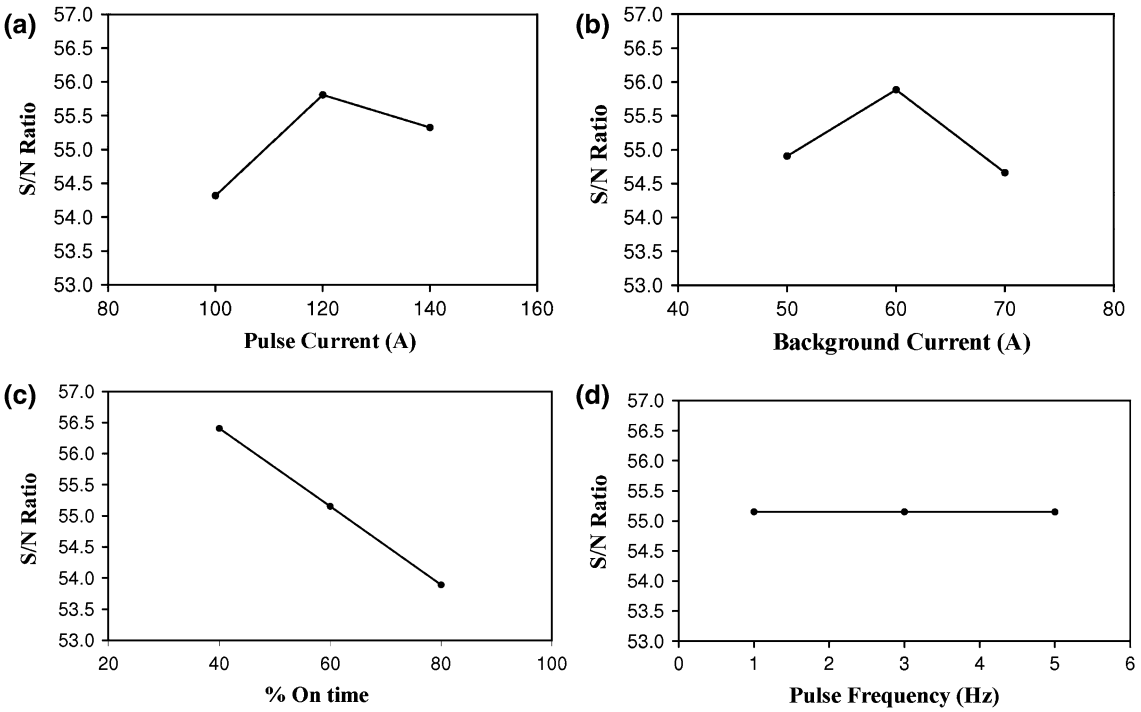

Fig. 3 The S/N response graphs for UTS to **a** pulse current, **b** background current, **c** % on time, and **d** pulse frequency

increases, sigma phase formation is favored. Figure 4 shows the microstructure of weld metal at trial no. 7, here, the low UTS (491 MPa) was observed. As shown in Fig. 4, the microstructure is characterized by a large amount of sigma phase at the α/γ interfaces. Table 5 shows the concentrations of major alloying elements in the ferrite, austenite, and sigma phases obtained from EDX analysis. In Fe–Cr–Ni systems, the sigma phase is a tetragonal

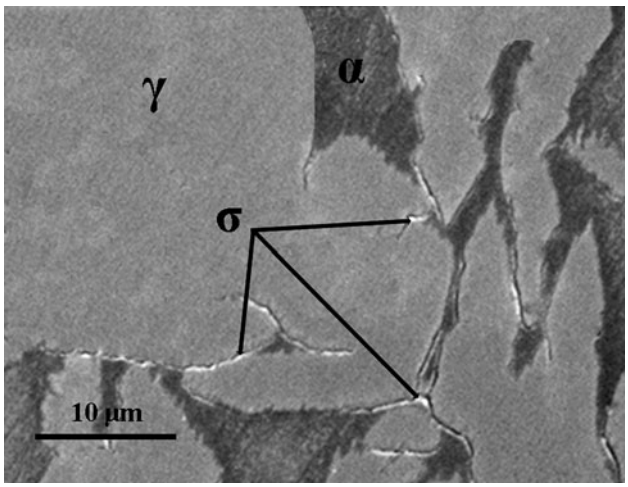

Fig. 4 SEM micrograph of UNS S32760 sample welded at trial no. 7 conditions

Table 5 Chemical composition of sigma and matrix phases determined by EDX analysis (wt.%)

Phase	Element			
	Chromium	Molybdenum	Nickel	Iron
γ (Austenite)	26.70	2.23	7.55	63.52
α (Ferrite)	30.22	2.60	5.82	61.36
σ (Sigma)	37.64	5.77	5.11	51.48

crystalline structure with 30 atoms per unit cell which contains Fe and Cr. The sigma phase content of this sample was measured to be approximately 25 vol.%. This sample (trial no. 7) exhibited low UTS due to the large amount of sigma phase in the microstructure and to the brittle nature and high hardness of this phase. The lack of formability of the sigma phase has been attributed to its low fraction or metallic binding [15–17]. Even a sigma concentration as low as 3 vol.% has been shown to reduce impact properties from 220 to 20 J at room temperature [18].

As shown in Eq. (1), the greater the S/N ratio the lesser the variance of UTS around the desired HB value [15]. In Table 4, A2, B2, C1, and D2 illustrate the largest values of S/N ratios for factors A, B, C, and D, respectively. In other words, based on the S/N ratio, the optimal parameters (conditions) for UTS are A at level 2, B at level 2, C at level 1, and D at level 2.

In addition to S/N ratio analysis, ANOVA was performed.

ANOVA was used to determine the influence and relative importance of the different factors. The sum of the square (SS), the degree of freedom (D), the variance (V), and the percentage of the contribution to the total variation (P) are four parameter symbols typically used in ANOVA, which can be calculated as shown in the following equations (Eqs. 2–6) [15]:

$$\mathrm{SS_T} = \sum_{i}^{m} \eta_i^2 - \frac{1}{m}\left[\sum_{i=1}^{m} \eta_i\right]^2, \tag{2}$$

where $\mathrm{SS_T}$ is the total sum of squares, m is the total number of the experiments, and η_i is the S/N ratio at the ith test.

$$\mathrm{SS_p} = \sum_{j=1}^{t} \frac{\left(S_{\eta_j}\right)^2}{t} - \frac{1}{m}\left(\sum_{i=1}^{m} \eta_i\right)^2, \tag{3}$$

where $\mathrm{SS_p}$ represents the sum of squares from the tested factors, p the one of the tested factors, j the level number of this specific factor p, t the repetition of each level of the factor p, and S_{η_j} the sum of the S/N ratio involving this factor and level j.

$$V_\mathrm{p}(\%) = \frac{\mathrm{SS_p}}{D_\mathrm{p}} \times 100, \tag{4}$$

where V_p is the variance from the tested factors, and D_p is the degree of freedom for each factor.

$$\mathrm{SS'_p} = \mathrm{SS_p} - D_\mathrm{p} V_\mathrm{e}, \tag{5}$$

where $\mathrm{SS'_p}$ represents the corrected sum of squares from the tested factors, and V_e the variance for the error.

$$P_\mathrm{p}(\%) = \frac{\mathrm{SS'_p}}{\mathrm{SS_T}} \times 100, \tag{6}$$

where P_p is the percentage of the contribution to the total variation of each individual factor.

The results of the ANOVA with the percentage contribution of each factor are illustrated in Table 6. As for the S/N ratio analysis, ANOVA analysis showed that pulse frequency was less effective than other parameters. Therefore, % on time, pulse current, and background current are found to be more effective. % on time has the maximal influence on the UTS with the 62.23% contribution followed by the pulse current with 21.13% and the background current with 16.18%. As shown in Table 6, it was observed that pulse frequency was an insignificant factor with only a 0.46% contribution.

In the ANOVA analysis, if the percentage error (P_e) contribution to the total variance is lower than 15%, no important factor is missing in the experimental design [15]. As shown in Table 6, the percentage error (P_e) is 0%. This indicates that no significant factors are missing in the experimental design.

In order to validate the methodology, confirmation tests should be performed at optimal process parameters to verify predicted results. If the predicted results are confirmed, the suggested optimum working conditions will be adopted [19].

Table 6 Results of the ANOVA for UTS

Symbol	Factors	Degree of freedom (D)	Sum of squares (SS)	Variance (V)	Corrected sums of squares (SS′)	Contribution (P, %)	Rank
A	Pulse current	2	13920.9	6960.4	13920.9	21.13	2
B	Background current	2	10656.9	5328.4	10656.9	16.18	3
C	% on time	2	40993.6	20496.8	40993.6	62.23	1
D	Pulse frequency	2	304.9	152.4	304.9	0.46	4
Error		0	0	0	0	0	
Total		8	65876.2			100	

Table 7 Evaluation of predicted UTS with experimental results of the confirmation experiment using optimal conditions

	Parameters				S/N ratio		Performance values for UTS (MPa)	
	A Pulse current, A	B Background current, A	C % on time	D Pulse frequency, Hz	Prediction	Experiment	Prediction	Experiment
Optimum level	2	2	1	2	57.7979	57.7185	776	769
Optimum value	120	60	40	3				

The predicted S/N ratio using the optimal level of the design parameters can be calculated as [15]

$$[\mathrm{S/N}]_{\mathrm{predicted}} = [\mathrm{S/N}]_m + \sum_{i=1}^{n} \left([\mathrm{S/N}]_i - [\mathrm{S/N}]_m\right), \quad (7)$$

where $[\mathrm{S/N}]_m$ is the total mean S/N ratio, $[\mathrm{S/N}]_i$ is the mean S/N ratio at the optimal level, and n is the number of the main design parameters that affect the quality characteristic.

The predicted S/N ratio using the optimal PCGTAW parameters for UTS can then be obtained and the corresponding UTS can also be calculated by using Eq. (1).

In the case of UTS, the value of $[\mathrm{S/N}]_m$ calculated from Table 3 is 55.1496. Also, $[\mathrm{S/N}]_i$ for A2, B2, C1, and D2 can be obtained from Table 4. The corresponding values are 55.8066, 55.8846, 56.4051, and 55.1504, respectively. By using these values, Eq. (7) can be written as $[\mathrm{S/N}]_{\mathrm{predicted}} = 55.1496 + [(55.8066 - 55.1496) + (55.8846 - 55.1496) + (56.4051 - 55.1496) + (55.1504 - 55.1496)]$. Therefore, the predicted S/N ratio (57.7979) for UTS can be obtained and the corresponding estimated UTS can also be calculated using Eq. (1). This means that the value of the S/N ratio (57.7979) at optimal condition (A2B2C1D2) is substituted into Eq. (1), and then Eq. (1) can be expressed as $57.7979 = -10 \log (1/y^2)$. Finally, the estimated UTS (776 MPa) can be obtained.

Table 7 shows the comparison of the predicted and the measured UTS values using the optimal conditions. There is a good agreement between the predicted and the experimental UTS values.

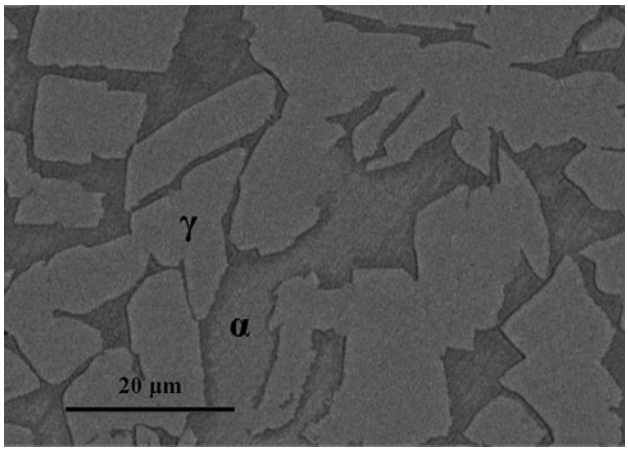

Fig. 5 SEM micrograph of the confirmation test using the optimized PCGTAW conditions

Figure 5 shows an SEM micrograph of the welded sample from the confirmation run. The best mechanical properties (such as UTS) of SDSS are obtained when the α/γ ratio is close to 50:50, and in the absence of intermetallic phases, such as sigma and chi [3]. As shown in Fig. 5, no precipitation or intermetallic phases appear on the micrograph and the microstructure consists of only ferrite

and austenite. Furthermore, the austenite content was 47%, which is very close to ideal value (50% austenite).

It can be speculated from the above discussions that Taguchi method as a design of experiments technique can be used to find optimum PCGTAW process parameters for the UTS of SDSS (UNS S32760) welds.

Conclusions

The influence of pulsed welding parameters, such as pulse current, background current, % on time, and frequency, on UTS of SDSS (UNS S32760) weldments was studied. It was found that % on time was the most significant PCGTAW process parameter. This parameter showed the highest percentage contribution (calculated percent contribution, $P = 62.23\%$) among the process parameters. The pulse current (calculated percent contribution, $P = 21.13\%$) was the second most-effective parameter. The next significant parameters were background current (16.18%) and pulse frequency (0.46%), respectively. The optimum conditions for UTS were achieved at a pulse current of 120 A, background current of 60 A, % on time of 40 and pulse frequency of 3 Hz. The confirmation tests showed that there is a good agreement between predicted (776 MPa) and measured (769 MPa) UTS results at optimum condition. Consequently, the Taguchi method provides a systematic and efficient methodology for the design optimization of the PCGTAW parameters on the UTS of SDSS weldments.

References

1. S.S.M. Tavares, J.M. Pardal, L.D. Lima et al., Characterization of microstructure, chemical composition, corrosion resistance and toughness of a multipass weld joint of superduplex stainless steel UNS S32750. Mater. Charact. **58**, 610–616 (2007)
2. M. Yousefieh, M. Shamanian, A. Saatchi, Influence of heat input in pulsed current GTAW process on microstructure and corrosion resistance of duplex stainless steel welds. J. Iron Steel Res. Int. **18**(9), 65–69 (2011)
3. M. Yousefieh, M. Shamanian, A. Saatchi, Optimization of experimental conditions of the pulsed current GTAW parameters for mechanical properties of SDSS UNS S32760 welds based on the Taguchi design method. J. Mater. Eng. Perform. (2011). doi: 10.1007/s11665-011-0105-z
4. J.M. Pardal, S.S.M. Tavares, M. Cindra Fonseca et al., Influence of the grain size on deleterious phase precipitation in superduplex stainless steel UNS S32750. Mater. Charact. **60**, 165–172 (2009)
5. M. Yousefieh, M. Shamanian, A. Saatchi, Influence of step annealing temperature on the microstructure and pitting corrosion resistance of SDSS UNS S32760 welds. J. Mater. Eng. Perform. **20**(9), 1678–1683 (2011)
6. S.H. Wang, P.K. Chiu, J.R. Yang, J. Fang, Gamma (γ) phase transformation in pulsed GTAW weld metal of duplex stainless steel. Mater. Sci. Eng., A **420**, 26–33 (2006)
7. A.A. Gokhale, D.J. Tzavaras, H.D. Brody, et al., Grain structure and hot cracking in pulsed current GTAW of AISI 321 stainless steel, in *Proceedings of Conference on Grain Refinement in Casting and Welds* (TMS-AIME, St. Louis, 1982) pp. 223–247
8. International Molybdenum Association, *Practical Guidelines for the Fabrication of Duplex Stainless Steels* (International Molybdenum Association, London, 1999)
9. P.J. Ross, *Taguchi Techniques for Quality Engineering* (McGraw-Hill, New York, 1988)
10. C. Montgomery Douglas, *Design and Analysis of Experiments* (Wiley, New York, 1997)
11. S. Madhav Phadke, *Quality Engineering Using Robust Design* (Prentice Hall, Englewood Cliffs, 1989)
12. A. Kumar, S. Sundarrajan, Selection of welding process parameters for the optimum but joint strength of an aluminum alloy. Mater. Manuf. Process. **21**, 789–793 (2006)
13. M. Hesampour, A. Krzyzaniak, M. Nyström, The influence of different factors on the stability and ultrafiltration of emulsified oil in water. J. Membr. Sci. **325**, 199–208 (2008)
14. S.M. Mousavi, S. Yaghmaei, A. Jafari et al., Optimization of ferrous biooxidation rate in a packed bed bioreactor using Taguchi approach. Chem. Eng. Process. **46**, 935–940 (2007)
15. M. Yousefieh, M. Shamanian, A. Saatchi, Optimization of the pulsed current gas tungsten arc welding (PCGTAW) parameters for corrosion resistance of super duplex stainless steel (UNS S32760) welds using the Taguchi method. J. Alloys Compd. **509**, 782–788 (2011)
16. R. Badji, M. Bouabdallah, B. Bacroix et al., Phase transformation and mechanical behavior in annealed 2205 duplex stainless steel welds. Mater. Charact. **59**, 447–453 (2008)
17. M. Pohl, O. Storz, T. Glogowski, Effect of intermetallic precipitations on the properties of duplex stainless steel. Mater. Charact. **58**, 65–71 (2007)
18. M. Martins, L.C. Casteletti, Microstructural characteristics and corrosion behavior of a super duplex stainless steel casting. Mater. Charact. **60**, 150–155 (2009)
19. Z. Beril Gonder, Y. Kaya, I. Vergili, H. Barlas, Optimization of filtration conditions for CIP wastewater treatment by nanofiltration process using Taguchi approach. Sep. Purif. Technol. **70**, 265–273 (2010)